Journal of Neuroscience Research 85:3642–3651 (2007)

In Vitro Neural Injury Model for Optimization of Tissue-Engineered Constructs

D. Kacy Cullen, Sarah E. Stabenfeldt, Crystal M. Simon, Ciara C. Tate, and Michelle C. LaPlaca*

Wallace H. Coulter Department of Biomedical Engineering, Institute for Bioengineering and Bioscience, Laboratory for Neuroengineering, Georgia Institute of Technology/Emory University, Atlanta, Georgia

Stem cell transplantation is a promising approach for the treatment of traumatic brain injury, although the therapeutic benefits are limited by a high degree of donor cell death. Tissue engineering is a strategy to improve donor cell survival by providing structural and adhesive support. However, optimization prior to clinical implementation requires expensive and time-consuming in vivo studies. Accordingly, we have developed a three-dimensional (3-D) in vitro model of the injured host–transplant interface that can be used as a test bed for high-throughput evaluation of tissue-engineered strategies. The neuronal-astrocytic cocultures in 3-D were subjected to mechanical loading (inducing cell death and specific astrogliotic alterations) or to treatment with transforming growth factor-β1 (TGF-β1), inducing astrogliosis without affecting viability. Neural stem cells (NSCs) were then delivered to the cocultures. A sharp increase in the number of $TUNEL^+$ donor cells was observed in the injured cocultures compared to that in the TGF-β1-treated and control cocultures, suggesting that factors related to mechanical injury, but not strictly astrogliosis, were detrimental to donor cell survival. We then utilized the mechanically injured cocultures to evaluate a methylcellulose-laminin (MC-LN) scaffold designed to reduce apoptosis. When NSCs were codelivered with MC alone or MC-LN to the injured cocultures, the number of $caspase^+$ donor cells significantly decreased compared to that with vehicle delivery (medium). Collectively, these results demonstrate the utility of an in vitro model as a preanimal test bed and support further investigation of a tissue-engineering approach for chaperoned NSC delivery targeted to improve donor cell survival in neural transplantation.

Key words: transplantation; apoptosis; laminin; neural stem cells

Traumatic brain injury (TBI) is caused by physical deformation of the brain and may result in prolonged or permanent loss of sensory, motor, and/or cognitive functions (Dixon et al., 1999; Adelson et al., 2000; Fujimoto et al., 2004; Povlishock and Katz, 2005). Current treatments have had limited success at restoring function, largely because of the complexity and duration of the pathophysiological alterations involved. A primary physical insult to the brain immediately initiates neural cell death and dysfunction and translates into a series of secondary complications including excitotoxicity, inflammation, and blood–brain barrier breakdown. As a result, a hostile environment is created and may induce delayed cell death for months after the insult (Smith et al., 1997; Conti et al., 1998; Bramlett and Dietrich, 2002; Kochanek et al., 2002). Reactive gliosis may also ensue, initially involving the recruitment and activation of astrocytes, macrophages, and microglia and ultimately forming a glial scar, a physical and chemical barrier isolating acutely injured tissue from the surrounding parenchyma (Fawcett and Asher, 1999; McGraw et al., 2001). The glial scar consists of a meshwork of reactive hypertrophic astrocytes exhibiting increased expression of intermediate filaments [e.g., glial fibrillary acidic protein (GFAP)] and is rich in chondroitin-sulfate proteoglycans (CSPGs; Asher et al., 2000; McKeon et al., 1999). Thus, although TBI initiates an array of pathophysiological alterations, prominent features of the postinjury environment include local cell death and reactive astrogliosis (Hill et al., 1996; Fawcett and Asher, 1999; Morgenstern et al., 2002; Raghupathi, 2004).

Given the prolonged degenerative state and complex environmental alterations following TBI, it is likely that a sustained effort will be required to alleviate or reduce neurological disability. Cell transplantation has the potential to

Contract grant sponsor: NSF; Contract grant number: CAREER Award BES-0093830; Contract grant sponsor: NIH/NIBIB; Contract grant number: EB-001014; Contract grant sponsor: NSF; Contract grant number: EEC-9731643; Contract grant sponsor: NIH/NINDS; Contract grant number: NRSA 1 F31 NS054527.

*Correspondence to: Michelle C. LaPlaca, PhD, GT/Emory Coulter Department of BME, 313 Ferst Dr., Atlanta, GA 30332-0535.
E-mail: michelle.laplaca@bme.gatech.edu

Received 24 January 2007; Revised 19 March 2007; Accepted 21 May 2007

Published online 1 August 2007 in Wiley InterScience (www.interscience.wiley.com). DOI: 10.1002/jnr.21434

dynamically target a wide range of pathological manifestations over a prolonged period. Stem cell transplants may have the ability to replace the function of missing or damaged cells, play either a direct or indirect role in the reconstruction of damaged neural circuitry, and reduce secondary damage by providing bulk trophic support or mediating cell–cell repair (for a review, see Longhi et al., 2005). Although transplantation is a promising approach, therapeutic effects are currently limited by the large degree of donor cell death that occurs and a lack of integration with the host brain tissue (Kanelos and McDeavitt, 1998; Riess et al., 2002; Picard-Riera et al., 2004; Bakshi et al., 2005; Boockvar et al., 2005). The postinjury environment may cause donor cell death through activation of apoptotic signaling pathways (Bakshi et al., 2005; Boockvar et al., 2005; Shindo et al., 2006), yet the mechanisms for this have not been fully elucidated.

Tissue engineering is one strategy for improving donor cell survival by transplanting cells in a bioactive scaffold designed to provide structural and adhesive support while presenting prosurvival signaling cues. In this study, we utilized a bioactive scaffold comprising a methylcellulose (MC) backbone tethered to the extracellular matrix protein laminin (LN). The thermoreversible properties of MC allow for minimally invasive delivery to the injury cavity, whereas incorporation of LN provides bioadhesive ligands to improve donor cell survival (Leone et al., 2005). We have characterized the biocompatibility of MC, the material properties of the MC-LN scaffold, and neural cell survival and attachment in culture conditions (Tate et al., 2001, 2004; Stabenfeldt et al., 2006). Optimization of these tissue-engineered constructs requires a feedback-based engineering process to alter cell density, ligand concentration, and methylcellulose concentration. The presented in vitro injury model permits an empirical systematic evaluation of tissue-engineered construct in an injured environment in order to determine the factors that promote donor survival and support differentiation. Currently, in vivo models are commonly used to assess cellular transplantation after TBI; however, we selected this high-throughput and more easily controlled in vitro model, which can be used prior to more expensive and time-consuming in vivo testing.

The goals of this study were (1) to evaluate factors influencing donor cell survival and differentiation by transplanting neural stem cells into in vitro models of mechanically induced cell death and/or reactive astrogliosis and (2) to examine the utility of the mechanically injured test bed to assess acute donor cell survival when codelivered with a bioactive tissue-engineered scaffold. The results validate the use of this in vitro model for high-throughput assessment of transplantation strategies and suggest that tissue engineering is a promising approach for attenuating donor cell death in the hostile postinjury environment.

MATERIALS AND METHODS

Cell Culture Procedures and Experimental Treatments

All procedures involving animals were approved by the Institutional Animal Care and Use Committee of the Georgia Institute of Technology. All cell reagents were obtained from Invitrogen (Carlsbad, CA) or Sigma-Aldrich (St. Louis, MO) unless otherwise noted.

Neuronal Harvest. Neurons were isolated from embryonic day 17–18 rat fetuses. Dames were anesthetized using isoflurane. Following cesarean section, the fetuses were rapidly decapitated, and the brains were removed. The cerebral cortices were isolated in Hank's Balanced Salt Solution (HBSS) and digested with trypsin (0.25% + 1 mM EDTA) at 37°C for 10 min. The trypsin-EDTA was then removed, and the tissue was triturated in HBSS containing *DNase*I (0.15 mg/mL). The cells were centrifuged at 100*g* for 3 min, then resuspended in coculture medium [neurobasal medium (NBM) + 2% B-27 supplement + 1% G-5 formulation + 500 μM L-glutamine] immediately prior to three-dimensional (3-D) plating. B-27 is an established supplement for primary neuronal cultures (Brewer et al., 1993; Brewer, 1995), and G-5 is a supplement formulated for the growth of astrocytic cultures (1 μg/mL biotin, 0.5 μg/mL basic FGF, 1 μg/mL EGF, 5 mg/mL human transferrin, 500 μg/mL insulin, 0.36 μg/mL hydrocortisone, and 0.52 μg/mL selenite).

Astrocytic Harvest and Maintenance. Astrocytes were harvested from postnatal day 0–1 rat pups as previously described (McCarthy and de Vellis, 1980). The pups were anesthetized using isoflurane and rapidly decapitated, and the cerebral hemispheres were placed in sterile HBSS. The isolated cortices were minced, and the tissue fragments were digested in trypsin (0.25% + 1 mM EDTA) for 5–7 min at 37°C, followed by treatment with *DNase*I (0.15 mg/mL) and gentle mechanical trituration. Cells were then centrifuged at 100*g* for 3 min, dispersed in DMEM/F12 with 10% fetal bovine serum, and plated in a flask. Mechanical agitation was used to detach less adherent cell types after 24 and 72 hr, and on reaching about 90% confluency, the primary astrocyte culture was passaged for 4 weeks. Astrocytes were used between passages 4 and 12 for plating in 3-D cultures to acquire a nearly pure population (>95% type I astrocytes) and to permit "maturation" of the astrocyte phenotype (Smith et al., 1990; Passaquin et al., 1994).

3-D Neuronal-astrocytic Coculture Plating and Maintenance. Cocultures were plated in 3-D in custom-made cell culture chambers consisting of a glass coverslip below a silicone-based elastomer mold (cross-sectional area = 2 cm^2, Sylgard 184 and 186; Dow Corning, Midland, MI). Prior to plating, the chambers were pretreated with 0.05 mg/mL poly-L-lysine (PLL), followed by Matrigel® (0.5 mL/well at 0.6 mg/mL; Becton Dickinson Biosciences, Bedford, MA) in Neurobasal medium (each treatment > 4 hr). Neuronal-astrocytic cocultures were plated in 3-D at a 1:1 initial neuron: astrocyte ratio at a density of 2,500 cells/mm^3 in Matrigel® matrix (500–750 μm thick; final concentration 7.5 mg/mL). Coculture medium was added following matrix gelation. Cocultures were maintained at 37°C and 5% CO_2/95% humidified air. Medium was replaced after 24 hr and every 2 days thereafter. Experiments were initiated after 21 days in vitro (DIV), permitting neural network formation and neuronal maturation (as indicated by the expression of mature isoforms of cytoskeletal proteins, synaptic markers, and functional electrophysiological properties) and maintaining a high baseline

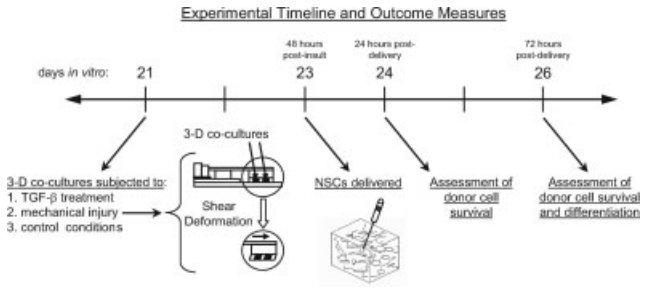

Fig. 1. Timeline of experiments and outcome measures. Neuronal-astrocytic cocultures in 3-D were plated in Matrigel® and at 21 DIV were subjected to treatment with TGF-β1 or to high-rate shear deformation or were left as uninjured controls. NSCs were delivered to these 3-D cocultures 48 hr postinsult, and donor cell survival and differentiation were subsequently assessed.

viability (>95%) in this 3-D coculture system (Ferreira et al., 1987; Nunez, 1988; Koller et al., 1990; Fletcher et al., 1991; Goedert et al., 1991; Pizzi et al., 1995; Steinschneider et al., 1996; Li et al., 1998; Evans et al., 1998). In addition, at an initial plating ratio of 1:1, astrocytic proliferation resulted in a relative reduction in neuronal presence to 10%–20% (occuring over 7–21 DIV; unpublished observations), a ratio of neurons to astrocytes more representative of that found in various cortical regions in vivo (Gabbott and Stewart, 1987; Braitenberg, 2001).

Mechanical Deformation and TGF-β1 Treatment. Neuronal-astrocytic cocultures were subjected to mechanical deformation, treatment with an astrogliosis-inducing cytokine, or control conditions. Cocultures were mechanically injured using a 3-D cell-shearing device (CSD), a custom-built electromechanical device capable of quantifiably imparting high-strain-rate shear deformation to 3-D-cell-containing matrices (LaPlaca et al., 2005; Cullen and LaPlaca, 2006). Immediately prior to injury, cultures were removed from the incubator and mounted in the device. The mechanical action of the device was driven by a linear-actuator (BEI Kimco, San Marcos, CA) governed by a custom-fabricated digital proportional-integral-derivative controller (25 kHz sampling rate, 16-bit sampling resolution) with closed-loop motion control feedback from an optical position sensor (RGH-34, 400-nm resolution; Renishaw, New Mills, UK). A symmetrical trapezoidal input was provided by code written in LabVIEW® (version 6.1; National Instruments, Austin, TX). Rapid horizontal motion of the cell chamber top plate relative to the fixed base of the cell chamber imparts high-strain-rate simple shear deformation to the 3-D-cell-containing matrices. This 3-D bulk shear deformation results in the generation of heterogeneous local cellular strains (Cullen and LaPlaca, 2006) where acute biophysical responses and longer-term cell survival each depend significantly on strain rate (LaPlaca et al., 2005), which is characteristic of traumatic loading in vivo (Margulies et al., 1990; Meaney et al., 1995). Figure 1 shows the 3-D cocultures subjected at 21 DIV to high-rate deformation (shear strain 0.50, loading onset time 16.6 msec, resulting strain rate 30 s^{-1}; $n = 33$), which produced significant cell death in 3-D neuronal cultures (Cullen and LaPlaca, 2006) and 3-D cocultures, or left as undeformed control cultures (uninjured control, $n = 32$). After exposure to mechanical deformation or control conditions, warm medium was added, and the cultures were returned to the incubator. Also beginning at 21 DIV, a set of cocultures were treated with transforming growth factor-β1 (TGF-β1; 10 ng/mL diluted in coculture medium), a cytokine previously demonstrated to induce astrogliotic alterations ($n = 21$; Logan et al., 1994). TGF-β1-treated cultures served as an experimental control representing TBI-induced astrogliotic alterations without the effects of neural cell death, allowing us to isolate the effects of astrogliosis on NSC responses following transplantation.

Neural Stem Cell Harvest and Maintenance. The neural stem cell was chosen as the donor cell phenotype on the basis of its ability to differentiate into the major cells of the CNS (neurons, astrocytes, and oligodendrocytes), a potential advantage when more than one cell type may be needed to mediate recovery of injured tissue (Rao, 1999; Whittemore, 1999; Gage, 2000). Primary fetal-derived green fluorescent protein–positive (GFP^+) NSCs were used to aid in posttransplant identification. Pregnant transgenic B6-TgN(β-act-EGFP)-osbY01 mice (C57BL6 background, a gift of Dr. Masaru Okabe) were anesthetized with isoflurane and sacrificed, and then embryos (gestational day 14.5) were isolated by cesarean section. The germinal zone was isolated and mechanically dissociated in HBSS. Cells were maintained in suspension culture in serum-free DMEM/F12 containing insulin (25 μg/mL), transferrin (100 μg/mL), putrescine (60 μM), sodium selenite (30 nM), progesterone (20 nM), and glucose (6 μg/mL). Human recombinant basic fibroblast growth factor (bFGF, 20 ng/mL) was added fresh every other day to maintain the cells as proliferating neurospheres, which were passaged every 7–10 days. Neurospheres used in the experiments were between passages 3 and 6.

Methylcellulose-laminin Scaffold. Methylcellulose (MC; M_w = 40 kDa) gels were prepared in 1× Dulbecco's phosphate-buffered saline (D-PBS) according to a dispersion technique previously reported (Kobayashi et al., 1999; Tate et al., 2001). Tethering of laminin-l (LN) to MC was accomplished via the photocrosslinker *N*-sulfosuccinimidyl-6-[4′-azido-2′-nitrophenylamino] hexanoate (sulfo-SANPAH; Pierce Biotechnology, Inc, Rockford, IL). Briefly, LN (200 μg/mL) was incubated with a 0.5 mg/mL sulfo-SANPAH solution in the absence of light for 2.5 hr. Residual unreacted sulfo-SANPAH was removed with microcentrifuge filters. LN-SANPAH (200 μg/mL) was reconstituted and thoroughly mixed on ice with MC (6.75% w/v). A thin layer of the MC+LN mixture was then cast on a glass slide and exposed to UV light for 4 min (100 W, 365 nm; BP-100AP lamp, UVP, Upland, CA) in order to initiate the photocrosslinking reaction. On completion of the tethering scheme, unbound LN was removed by rinsing with D-PBS supplemented with 0.1% Tween-20, followed by three rinses with D-PBS. MC tethered to LN is referred to as MC-LN, and untreated MC is referred to as MC.

Delivery of NSCs to 3-D Neuronal-astrocytic Cocultures. NSCs were delivered via controlled injection designed to mimic in vivo transplant protocols implemented by our group (Tate et al., 2002; Shear et al., 2004). In a laminar flow hood, a micromanipulator was fixed to a stereoscope base to visualize the injection. Forty-eight hours following exposure to mechanical loading (23 DIV; see Fig. 1), the TGF-β1 treatment, or control conditions, most of the medium was

removed (leaving 100 μL). NSCs were then delivered to the 3-D neuron-astrocyte cocultures using a microsyringe (Hamilton, 10 μL) gradually penetrating to a depth of 200 μm below the coculture surface. The delivery consisted of 2.5 μL containing 1.5×10^4 cells [dispersed in media (vehicle: NBM/B-27/L-glutamine), MC, or MC-LN] delivered over 1.5–2.0 min. The cultures were returned to a tissue culture incubator for 60 min, after which NBM/B-27/L-glutamine was added.

Assessment of Cell Viability/Cytotoxicity, TUNEL Staining, and Caspase Activation

Cell viability/cytotoxicity. Coculture viability was assessed following exposure to mechanical loading, TGF-β1 treatment, or control conditions using probes to distinguish live and dead cells (n = 5–7 cocultures per group). Two days following insult, cocultures were incubated with 4 μM ethidium homodimer-1 and 2 μM calcein AM (Molecular Probes, Eugene, OR) at 37°C for 30 min and then rinsed with 0.1M D-PBS. The numbers of viable and dead cells were quantified (3–5 randomly selected regions per culture).

TUNEL. Terminal deoxynucleotidyl transferase (TdT)–mediated dUTP nick-end labeling (TUNEL) assay was used to assess DNA fragmentation and strand breaks, indicative of cell death, in transplanted cells 24 and 72 hr postdelivery (n = 3–5 cocultures per group, each stained in triplicate). The 3-D neural cocultures containing transplanted GFP^+ cells were fixed with 3.7% formaldehyde (Fisher, Fairlawn, NJ) for 60 min and then placed in 30% sucrose (Sigma-Aldrich) overnight at 4°C. Cocultures were then placed in Optimum Cutting Temperature embedding compound (Sakura, Tokyo, Japan), flash-frozen in liquid nitrogen, sectioned on a cryostat (20 μm thick; Microm Cryo-Star, Walldorf, Germany), and mounted on glass slides. Sections containing GFP^+ cells were stained using a commercially available TUNEL kit (NeuroTACS™ II; Trevigen, Gaithersburg, MD). Briefly, cells were permeabilized using NeuroPore™ for 30 min at 18°C–24°C. After rinsing, slides were immersed in TdT-labeling buffer for 5 min, followed by the addition of labeling reaction mix (containing TdT dNTP mix, Mn^{2+}, and TdT enzyme in labeling buffer) for 60 min humidified at 37°C. Next, the slides were immersed in a TdT stop buffer, followed by rinsing, and strep-HRP was added for 10 min humidified at 18°C–24°C. After rinsing, the slides were immersed in a DAB solution for 4 min followed by counterstaining. Microscopic analysis was performed to determine the number of $TUNEL^+$ nuclei colocalized with GFP.

Caspase Activation. The level of activated caspases, a family of proteolytic enzymes central in apoptotic cell death, was measured in order to assess the involvement of proapoptotic pathways in NSCs transplanted into injured 3-D cultures using a commercially available kit (CaspaTag™ Pan-Caspase Assay; Chemicon, Temecula, CA; n = 3–4 cocultures per condition). The reagent solution, which uses a sulforhodamine-labeled fluoromethyl ketone peptide inhibitor of caspase (SR-VAD-FMK) to covalently bind the activated caspase heterodimer, was mixed in media (1:30) and added to the cocultures. Following incubation at 37°C at 5% CO_2 for 60 min, the cocultures were rinsed. The binding reaction causes the fluorescent indicator to be retained in a cell on rinsing, thus permitting fluorometric detection of activated caspases colocalized with GFP^+ cells in 3-D cocultures (4–5 randomly selected regions per coculture were sampled).

Immunocytochemistry. Immunocytochemistry was employed to assess (1) reactive astrogliosis in mechanically injured, TGF-β1-treated, and control cocultures and (2) NSC differentiation following delivery to injured, treated, or control cocultures. The 3-D cocultures (with or without NSCs) were fixed, cryoprotected, embedded, frozen, and sectioned as described for the TUNEL assay. Sections were rinsed in PBS and permeabilized using 0.3% Triton X100 (Kodak, Rochester, NY) + 8% goat serum (Invitrogen) for 60 min. Primary antibodies were added (in PBS + 0.1% Triton X100 + 2% serum) overnight at 4°C in a humidified chamber. After rinsing, the appropriate secondary fluorophore-conjugated antibodies (FITC/TRITC-conjugated IgG, Jackson Immuno Research, or Alexa 488/546-conjugated IgG, Molecular Probes) were added (in PBS + 2% serum) for 2 hr at 18°C–24°C in a humidified chamber. For assessment of astrogliosis, sections were immunostained using primary antibodies recognizing: (1) GFAP (AB5804 or MAB360, 1:400, Chemicon), (2) CS-56 (a general CSPG marker; C8035, 1:100, Sigma), and (3) neurocan (a specific CSPG; MAB5212, 1:1,000, Chemicon), with n = 3–5 cocultures per group per marker with each sample stained in triplicate. For analysis of NSC differentiation patterns, sections containing GFP^+ cells were selected and immunostained using primary antibodies for (1) GFAP (MAB360, 1:400), (2) Tuj-1 (βIII-tubulin; MMS-435P, 1:2,000, Covance, Denver, PA), (3) neuronal-glial antigen-2 (NG2; AB5320, 1:200, Chemicon), and (4) nestin (MAB353, 1:200, Chemicon), with n = 3–4 cocultures per group with each sample stained in triplicate. NSC phenotypic expression was assessed via colocalization of GFP with the primary/TRITC or Alexa 546–conjugated secondary antibody specific for a particular marker. In all cases, counterstaining was performed using Hoechst 33258 (1:1,000, Molecular Probes).

Data Collection and Statistical Analysis

For cell viability and caspase activation assays, intact (full-thickness) cocultures were viewed using a confocal laser-scanning microscope (LSM 510; Zeiss, Oberkochen, Germany) and z-stacks (50 μm) were analyzed to distinguish individual cell bodies using LSM Image Browser (Zeiss) and projected as 2-D images for visualization. For immunocytochemistry and TUNEL, coculture sections were viewed using brightfield, phase-contrast, and/or fluorescent microscopy techniques (Eclipse TE300 or Eclipse 80i; Nikon, Melville, NY) with images digitally captured and analyzed using Image-Pro Plus (Media Cybernetics, Silver Spring, MD). Data are presented as the mean ± standard deviation. To analyze potential alterations in CSPG presence following experimental conditions, the mean image intensity was quantified using Image Pro Plus based on zero intensity assigned to sections only exposed to secondary fluorescent antibodies. To characterize the 3-D coculture environment, general-linear-model ANOVA was used with 3-D coculture treatment (control, TGF-β1 treated, or

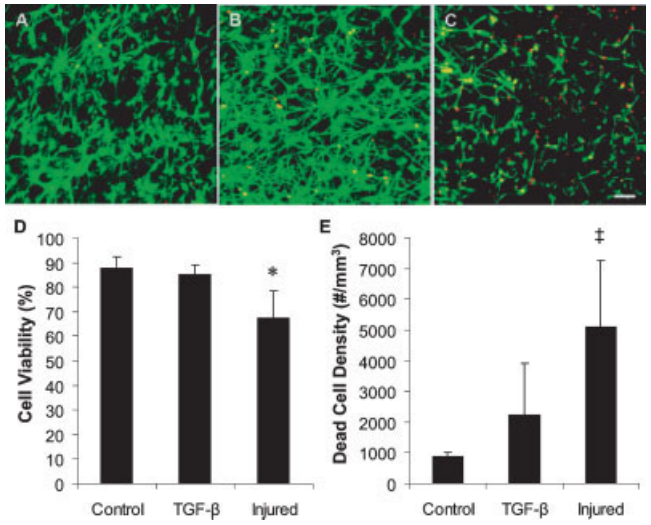

Fig. 2. Coculture viability following mechanical deformation or TGF-β1 treatment. The 3-D neuronal-astrocytic cocultures were subjected to mechanical loading, TGF-β1 treatment, or control conditions at 21 DIV, and culture viability was assessed 48 hr later. Fluorescent confocal reconstructions of representative cocultures after (**A**) control conditions, (**B**) TGF-β1 treatment, or (**C**) mechanical injury (scale bar = 50 μm). **D:** Mechanical loading resulted in a significant reduction in culture viability, whereas cytokine treatment had no effect on culture viability ($^{\star}P < 0.05$). **E:** High-rate deformation resulted in a significant increase in the density of dead cells ($^{\ddagger}P < 0.05$). [Color figure can be viewed in the online issue, which is available at www.interscience.wiley.com.]

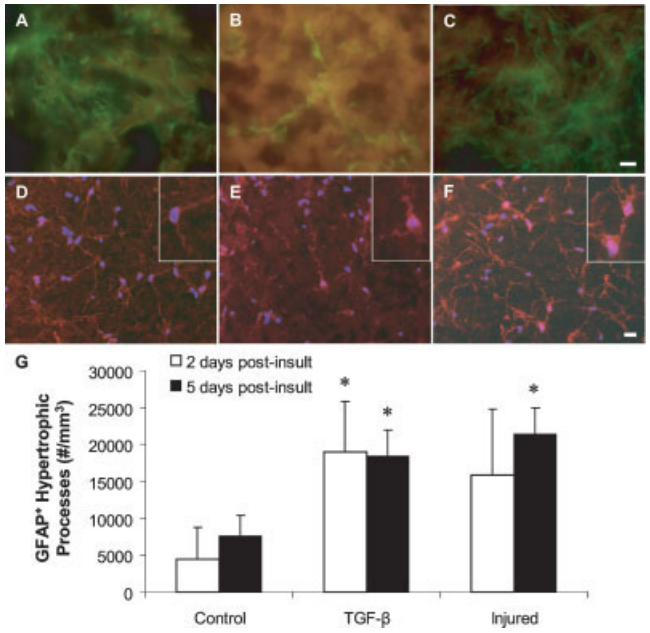

Fig. 3. CSPG expression and astrocyte hypertrophy following mechanical injury or TGF-β1 treatment. Representative fluorescent micrographs of neuronal-astrocytic cocultures exposed to (**A, D**) control conditions, (**B, E**) TGF-β1 treatment, or (**C, F**) mechanical injury (scale bar = 20 μm). **A–C:** Cocultures immunolabeled for neurocan (red) and GFAP (green) with nuclear counterstain (blue) 2 days postinsult. Expression of CSPGs, including neurocan, significantly increased following TGF-β1 treatment ($P < 0.05$). **D–F:** Cocultures immunolabeled for GFAP (red) with nuclear counterstain (blue) 5 days postinsult. **H:** Density of $GFAP^{+}$ hypertrophic processes (insets in **D–F**) significantly increased beyond control levels 2 and 5 days following TGF-β1 treatment and by 5 days following mechanical injury ($^{\star}P < 0.05$). [Color figure can be viewed in the online issue, which is available at www.interscience.wiley.com.]

mechanically injured) as the independent variable and culture viability or astrogliotic parameter as the dependent variable. For NSC interface studies, general-linear-model ANOVA was used with 3-D coculture treatment, delivery (vehicle, MC, or MC-LN), and time postdelivery (24 or 72 hr) as independent variables and donor cell outcomes as dependent variables ($TUNEL^{+}$, $caspase^{+}$, phenotype, process outgrowth). GFP+ donor cell integration in the host 3-D cocultures was quantified by counting cells that had extending neurites >10 μm and expressing this quantity as a percentage of total cells. When significant differences were found between groups, post hoc Tukey's pairwise comparisons were then performed. For all statistical tests, a P value <0.05 was required for differences to be considered significant.

RESULTS

High-Rate Mechanical Loading Resulted in Localized Cell Death and Developing Astrogliosis in 3-D Neuronal-Astrocytic Cocultures

Neuronal-astrocytic cocultures exhibited widespread 3-D process outgrowth and consisted of astrocytes and functional neurons at 21 DIV. At this point, the cultures were subjected to high-rate shear deformation, to treatment with TGF-β1, or were left untreated as controls, with viability and markers of astrogliosis subsequently assessed. Forty-eight hours postinsult, fluorescent confocal microscopy revealed a significant decrease in the percentage of viable cells with a concurrent increase in the spatial density of dead cells following mechanical loading ($P < 0.05$ each). In addition, at this time, most of the dead or dying cells were neurons rather than astrocytes, as assessed by immunocytochemistry for phenotypic markers (data not shown). However, treatment with TGF-β1 did not significantly affect coculture viability (Fig. 2). Characteristics of reactive astrogliosis were evaluated via immunocytochemistry using markers for GFAP and CSPGs. By 48 hr postinsult, the matrix content of CSPGs, specifically neurocan, increased precipitously following TGF-β1 treatment compared to in the controls ($P < 0.05$); however, significant alterations in matrix CSPG content were not observed following exposure to the mechanical loading regime used in this study (Fig. 3). In addition, astrocytic reactivity and hypertrophy were evaluated by assessing GFAP expression (Fig. 3). There was an increase in both the intensity of GFAP immunoreactivity and in process density following TGB-β1 treatment or mechanical injury compared to in the controls (Fig. 3). Specifically, there were signif-

icant increases in the density of hypertrophic processes by 2 days following treatment with TGF-β1 ($P < 0.05$). However, such alterations in the density of $GFAP^+$ hypertrophic processes manifested over a longer period following high-rate deformation as a significant increase beyond control levels was not observed until 5 days postinsult ($P < 0.05$). The delayed increase in the density of $GFAP^+$ hypertrophic processes may have been a result of cell death following injury, causing recovery time for the process density to increase beyond preinjury levels. Thus, TGF-β1 treatment induced a robust astrogliotic response consisting of increased GFAP expression, astrocyte hypertrophy, and increased matrix CSPG expression, specifically neurocan, without influencing culture viability. Alternatively, mechanical injury induced significant cell death with a delayed increase in hypertrophic process density.

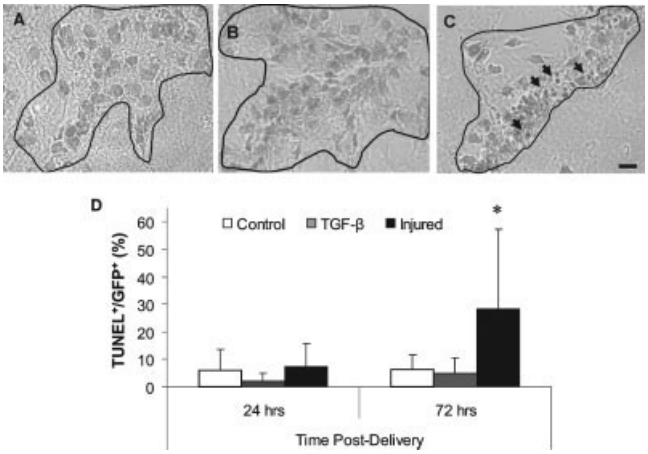

Fig. 4. Donor cell survival following vehicle delivery. Photomicrographs of GFP^+ donor cells 72 hr after delivery to 3-D cocultures subjected to (**A**) control conditions, (**B**) TGF-β1 treatment, and (**C**) mechanical injury ($TUNEL^+$ nuclei appear brown). Scale bar = 10 μm. **D:** $TUNEL^+/GFP^+$ donor cells were quantified 24 and 72 hr postdelivery. Percentage of $TUNEL^+$ donor cells did not significantly differ between the coculture groups 24 hr following delivery. However, by 72 hr following delivery, significantly more $TUNEL^+$ donor cells were observed in the mechanically injured 3-D cocultures than in the control and TGF-β1-treated cocultures ($*P < 0.05$).

Factors in a Mechanically Injured but Not a TGF-β1-Treated Environment Were Detrimental to NSC Survival without Influencing Differentiation Patterns

NSCs in vehicle (medium) were delivered to mechanically injured, TGF-β1-treated, or control cocultures 48 hr postinsult to test the effects of injured and/or reactive astrogliotic environmental parameters on NSC survival and differentiation (Fig. 1). TUNEL staining, which labels the fragmented DNA of dying cells, was used to assess donor cell survival 24 and 72 hr following delivery. There was a paucity of $TUNEL^+$ donor cells in the mechanically injured, TGF-β1-treated, and control 3-D cocultures 24 hr following delivery. Approximately 5% of the donor cells in each of these groups were $TUNEL^+$, with no statistical difference in the percentage of $TUNEL^+/GFP^+$ cells at this time (Fig. 4). Seventy-two hours following delivery, the pattern of $TUNEL^+/GFP^+$ cells remained unchanged in the control and TGF-β1-treated cocultures; however, there was a sharp increase in the percentage of $TUNEL^+$ donor cells delivered to mechanically injured 3-D cocultures, which rose to nearly 30% ($P < 0.05$). There were often clusters of GFP^+ cells in mechanically injured cocultures that presented a relatively large number of dying donor cells (Fig. 4C). Thus, there was an increase in $TUNEL^+$ donor cells when delivered to a mechanically injured environment compared to in the control and cytokine-induced astrogliotic cocultures.

The expression of specific neural phenotypic markers was assessed 72 hr following transplantation using immunocytochemistry. Morphological indications of donor cell growth and process extension in the host coculture were evident in many cases. In each of the coculture treatment groups, GFP^+ cells were colabeled with nestin (intermediate filament found in undifferentiated NSCs), GFAP (intermediate filament expressed by astrocytes), NG2 (transmembrane CSPG expressed by various neural subtypes, often used as a marker for oligodendrocyte precursors), or Tuj-1 (intermediate filament expressed by immature neurons). Donor cells most prominently expressed GFAP, followed by nestin, NG2, and Tuj-1 (Fig. 5). However, there was not a significant difference in the differentiation profiles of donor cells delivered to the different coculture conditions.

NSCs Codelivered in Tissue-Engineered Scaffolds Resulted in Reduced Caspase Activation in Mechanically Injured 3-D Cocultures

On the basis of our finding that elements in a mechanically injured but not a strictly astrogliotic environment detrimentally influenced NSC survival, we tested the hypothesis that tissue-engineered scaffolds with prosurvival bioadhesive ligands would enhance NSC survival in a surrogate postinjury environment. Accordingly, NSCs were delivered to mechanically injured or control 3-D cocultures with no scaffold (media vehicle), in a MC-only scaffold, or in a MC-LN scaffold. In this study, caspase activation was evaluated to detect early markers of donor cell death via caspase-related apoptotic mechanisms. Assessment 72 hr postdelivery revealed that donor cell caspase activation depended significantly on the coculture environment (injured vs. control; $P < 0.01$) or the delivery method (vehicle vs. MC vs. MC-LN; $P < 0.01$) or interactions of these variables ($P < 0.05$), indicating that effects of delivery platform depended on the coculture environment (Fig. 6). When NSCs were delivered with media vehicle only, there was a significant increase in the percentage of donor cells with colocalized GFP and acti-

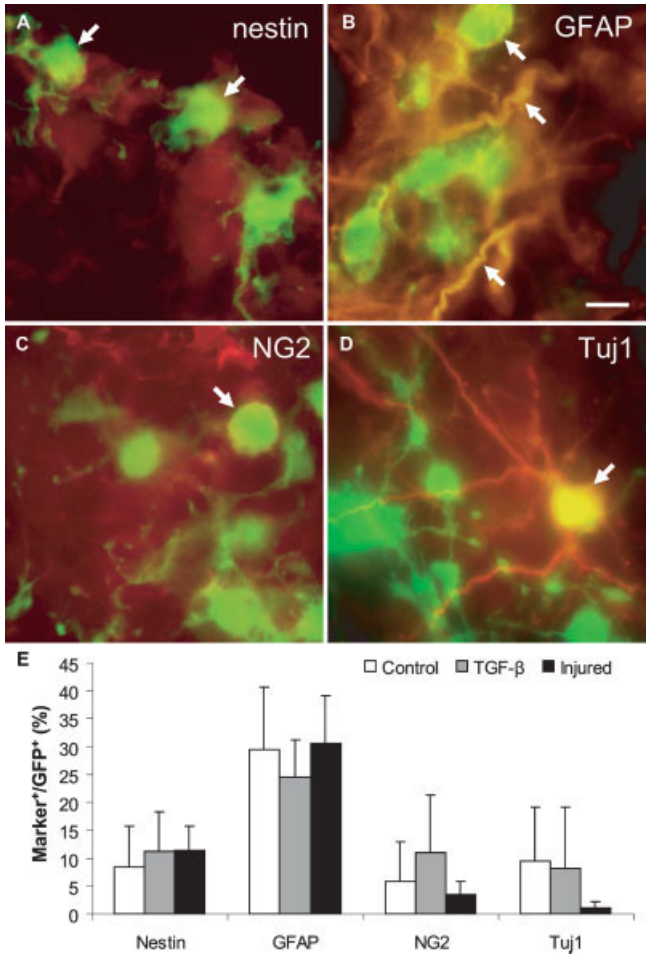

Fig. 5. Donor cell differentiation profiles following vehicle delivery. Donor cells were immunolabeled for specific phenotypic markers 72 hr following delivery to mechanically injured, TGF-β1 treated, or control 3-D cocultures. GFP^+ cells were found that coexpressed (**A**) nestin, (**B**) GFAP, (**C**) NG2, and (**D**) Tuj-1. Scale bar = 10 μm. **E:** Donor cells most prominently differentiated along an astrocytic lineage; however, expression profiles of NSCs delivered to the different coculture groups did not significantly differ. [Color figure can be viewed in the online issue, which is available at www.interscience.wiley.com.]

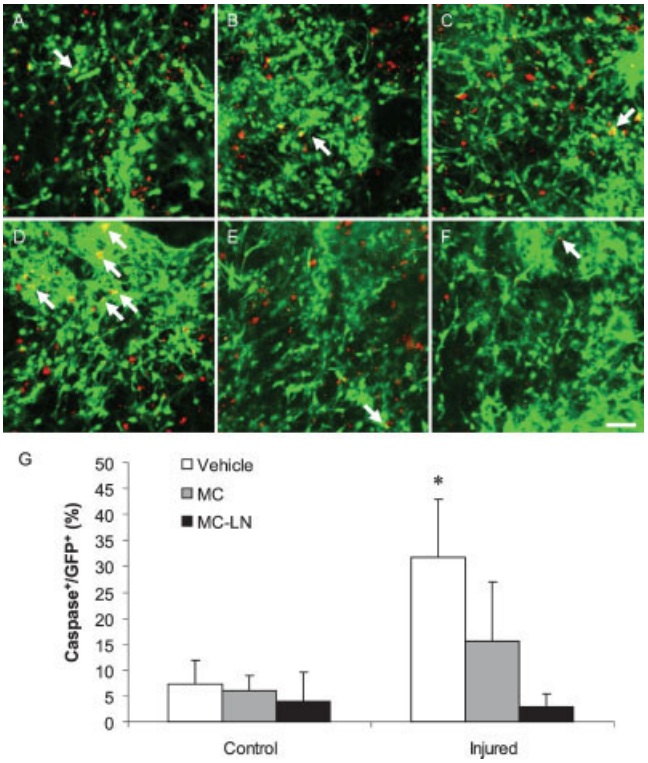

Fig. 6. Donor cell survival when delivered with a MC-LN tissue engineered construct. GFP^+ NSCs were codelivered with media (vehicle), MC, or MC-LN to 3-D cocultures after exposure to control conditions or to mechanical injury, and caspase activity (red) was assessed 74 hr postdelivery. Representative confocal reconstructions of GFP^+ donor cells in (**A, D**) vehicle, (**B, E**) MC, or (**C, F**) MC-LN in 3-D cocultures following exposure to control conditions (**A–C**) or mechanical injury (**D–F**). **G:** When NSCs were delivered with vehicle to the injured cocultures, the percentage of cells with colocalized GFP and activated caspases significantly increased beyond control levels ($^*P < 0.05$). However, delivery in MC-LN and MC mitigated this effect. NSCs codelivered in MC-LN to injured cocultures reduced activated caspases to levels near donor cells in control cocultures. [Color figure can be viewed in the online issue, which is available at www.interscience.wiley.com.]

vated caspases in mechanically injured versus in control 3-D cocultures ($P < 0.05$). As expected, the mean percentage of GFP^+ cells with activated caspases was similar to the mean percentage of GFP^+ cells that were also $TUNEL^+$, supporting our previous findings and also indicating these cells are dying by apoptosis (Fig. 6). In control cocultures, the presence of MC or MC-LN did not significantly alter the $GFP^+/caspase^+$ colocalization from levels attained from vehicle delivery. Alternatively, in injured cocultures, the presence of MC or MC-LN resulted in a significant decrease in the amount of $GFP^+/caspase^+$ colocalized ($P < 0.05$ and $P < 0.001$, respectively) compared to in the vehicle. These results suggest that both MC and MC-LN may reduce the effects of the injured environment on caspase activation.

In addition, the percentage of donor cells extending processes was quantified, revealing that more than 50% of the donor cells delivered in MC-LN and 40% of donor cells delivered in MC were extending processes (Fig. 6). Conversely, fewer than 25% of donor cells delivered with vehicle extended processes (MC-LN vs. vehicle; $P < 0.05$), suggesting that delivery in an MC-LN scaffold augmented donor cell integration. Thus, codelivery of NSCs with MC-LN scaffolds resulted in increased donor cell process outgrowth while reducing caspase activation of donor cells when delivered to injured cocultures.

DISCUSSION

We utilized a controlled 3-D in vitro injury model exhibiting cell death and markers of reactive astrogliosis to examine NSC survival following transplantation into this

surrogate injury environment. This study revealed that elements related to mechanical injury, but not strictly astrogliosis, negatively influence NSC survival at acute times following delivery. After characterizing the mechanically injured environment and establishing the baseline survival of NSCs, this in vitro model was utilized to evaluate the ability of a hydrogel MC-LN scaffold to chaperone NSCs into this injured/reactive environment. By codelivering the NSCs with a MC or MC-LN scaffold to mechanically injured cocultures, donor cell caspase activity was reduced, demonstrating the potential efficacy of tissue-engineered strategies to mitigate detrimental factors associated with mechanical injury.

Neural models have been developed designed to evaluate interfaces between various cell culture populations. For example, simple planar cultures with NSCs delivered above a confluent astrocyte monolayer (Faijerson et al., 2006) or cells placed above tissue slices (Tom et al., 2004). There are fundamental differences between these test environments and 3-D interfaces as both cell–cell and cell–matrix interactions (e.g., receptor profiles and distribution) differ markedly (Cukierman et al., 2001, 2002; Schmeichel and Bissell, 2003; Yamada et al., 2003). Also, the local microenvironment may differ, as secreted and/or soluble factors may be diluted in the culture medium, whereas in 3-D they may be maintained locally or become matrix bound. Thus, the in vitro model presented in this article is a simplified yet versatile system to evaluate 3-D interactions between NSCs and an injured/reactive environment, which are crucial for the success of neurotransplantation.

NSC transplantation has been shown to mediate some neurological recovery in animal models of TBI (Riess et al., 2002; Lu et al., 2003; Shear et al., 2004), yet the efficacy has been plagued by poor donor cell survival (Kanelos and McDeavitt, 1998; Riess et al., 2002; Picard-Riera et al., 2004; Bakshi et al., 2005; Boockvar et al., 2005; Shindo et al., 2006). Our results support this hypothesis, as we found a nearly six-fold increase in donor cell death in injured cultures compared to in controls. Cell death of engrafted stem cells may possibly occur through apoptotic mechanisms. For example, caspase-mediated apoptosis in neural stem cells has been implicated in transplantation in the enteric nervous system (Micci et al., 2005) and in traumatic brain injury (Bakshi et al., 2005). The in vitro model presented in this article represents aspects of the in vivo setting and therefore can be used to optimize transplant conditions to overcome poor survival in a controlled manner. We hypothesized that a tissue-engineered construct containing a MC-LN scaffold would enhance NSC survival after delivery to a surrogate injured/reactive environment by providing both physical support and a bioactive substrate that promotes survival through adhesion to LN (Leone et al., 2005; Stabenfeldt et al., 2006). LN has been shown to be antiapoptotic in neurons after ischemic (Gu et al., 2005) and excitotoxic (Gary and Mattson, 2001; Gary et al., 2003) insults to the brain. A significant reduction in caspase activity was observed when NSCs were codelivered with MC-LN or MC compared to vehicle. These results demonstrate that the delivery microenvironment affects donor cell survival and that both structural and receptor-mediated interactions may be beneficial.

TGF-β1 treatment did not affect donor cell survival, suggesting that variables related to the neural response to mechanical injury, but not astrogliosis alone, lead to donor cell death. The detrimental effects of a postinjury environment may be caused by a variety of factors, such as local cell death and the release of neurotoxic chemicals (e.g., tumor necrosis factor-α and interleukins; McIntosh et al., 1999; Weber, 2004). Conversely, neurotrophic factors may increase following brain injury and support donor cell survival (Ray et al., 2002). Future studies utilizing this in vitro test bed may be suitable for isolating and systematically testing the effects of these parameters, leading to therapies aimed at altering host responses to promote transplant survival.

The differentiation profile of NSCs was assessed following delivery using a range of neural cell markers chosen based on in vitro and in vivo differentiation patterns (Riess et al., 2002; Shear et al., 2004; Tate et al., 2004; Shindo et al., 2006). Although different coculture microenvironments (e.g., host cell reactivity, cytokines, growth factors, matrix constituents) may influence NSC differentiation (Irvin et al., 2003; Mondal et al., 2004), no differences in the phenotypic profile of transplanted cells were observed between injured/reactive cocultures and controls. Most transplanted cells progressed along an astrocytic lineage ($GFAP^+$), in agreement with previous in vitro studies, in which NSCs primarily expressed GFAP following plating on LN-, fibronectin-, or collagen IV–coated surfaces (Tate et al., 2004). Also, a modest percentage of NSCs delivered to the cocultures progressed toward a neuronal phenotype ($Tuj\text{-}1^+$), and this neuronal yield was relatively high compared to that reported in other works (Santa-Olalla and Covarrubias, 1995; Tate et al., 2004). However, when NSCs were delivered on top of scratch-injured astrocytes, astrocytic differentiation was enhanced (Faijerson et al., 2006). Detectable phenotypic changes may take longer than 72 hr to manifest, or intrinsic differentiation patterns may outweigh the microenvironmental factors in this model. In addition, the baseline cellular constituents (e.g., neuron:astrocyte ratio) and matrix composition of the culture may influence the differentiation profile of donor cells and may be experimentally modified using this experimental platform.

In conclusion, this study has demonstrated the utility of a well-controlled 3-D in vitro model of neural injury to investigate prospective factors that influence NSC function, particularly survival. Future work will investigate additional injury-related factors that may influence NSCs, and such knowledge will aid in the optimization of tissue-engineered scaffolds to improve NSC survival, integration, and control of differentiation. Furthermore, the complexity of this model may be incrementally increased by adding other variables present

in vivo (e.g., microglia) in order to elucidate their influence on NSC survival and integration. As a consequence, this research may improve cell transplantation strategies and provide a mechanistic basis for the development of clinically effective treatments for TBI as well as other neurological disorders.

ACKNOWLEDGMENTS

The authors acknowledge Dr. Masaru Okabe (Osaka University, Osaka, Japan) for the generous donation of EGFP transgenic mice. The authors also thank Maggie Wolfson, Brock Wester, and Dr. Michael Schumm for technical contributions.

REFERENCES

Adelson PD, Dixon CE, Kochanek PM. 2000. Long-term dysfunction following diffuse traumatic brain injury in the immature rat. J Neurotrauma 17:273–282.

Asher RA, Morgenstern DA, Fidler PS, Adcock KH, Oohira A, Braistead JE, Levine JM, Margolis RU, Rogers JH, Fawcett JW. 2000. Neurocan is upregulated in injured brain and in cytokine-treated astrocytes. J Neurosci 20:2427–2438.

Bakshi A, Keck CA, Koshkin VS, LeBold DG, Siman R, Snyder EY, McIntosh TK. 2005. Caspase-mediated cell death predominates following engraftment of neural progenitor cells into traumatically injured rat brain. Brain Res 1065(1–2):8–19.

Boockvar JA, Schouten J, Royo N, Millard M, Spangler Z, Castelbuono D, Snyder E, O'Rourke D, McIntosh T. 2005. Experimental traumatic brain injury modulates the survival, migration, and terminal phenotype of transplanted epidermal growth factor receptor-activated neural stem cells. Neurosurgery 56(1):163–171; discussion 171.

Braitenberg V. 2001. Brain size and number of neurons: an exercise in synthetic neuroanatomy. J Comput Neurosci 10(1):71–77.

Bramlett HM, Dietrich WD. 2002. Quantitative structural changes in white and gray matter 1 year following traumatic brain injury in rats. Acta Neuropathol (Berl) 103:607–614.

Brewer GJ. 1995. Serum-free B27/neurobasal medium supports differentiated growth of neurons from the striatum, substantia nigra, septum, cerebral cortex, cerebellum, and dentate gyrus. J Neurosci Res 425: 674–683.

Brewer GJ, Torricelli JR, Evege EK, Price PJ. 1993. Optimized survival of hippocampal neurons in B27-supplemented Neurobasal, a new serum-free medium combination. J Neurosci Res 355:567–576.

Conti AC, Raghupathi R, Trojanowski JQ, McIntosh TK. 1998. Experimental brain injury induces regionally distinct apoptosis during the acute and delayed post-traumatic period. J Neurosci 18:5663–5672.

Cukierman E, Pankov R, Stevens DR, Yamada KM. 2001. Taking cell-matrix adhesions to the third dimension. Science 294:1708–1712.

Cukierman E, Pankov R, Yamada KM. 2002. Cell interactions with three-dimensional matrices. Curr Opin Cell Biol 14:633–639.

Cullen DK, LaPlaca MC. 2006. Neuronal response to high rate shear deformation depends on heterogeneity of the local strain field. J Neurotrauma 23:1304–1319.

Dixon CE, Kochanek PM, Yan HQ, Schiding JK, Griffith RG, Baum E, Marion DW, DeKosky ST. 1999. One-year study of spatial memory performance, brain morphology, and cholinergic markers after moderate controlled cortical impact in rats. Journal of Neurotrauma 16:109–122.

Evans MS, Collings MA, Brewer GJ. 1998. Electrophysiology of embryonic, adult and aged rat hippocampal neurons in serum-free culture. J Neurosci Methods 79(1):37–46.

Faijerson J, Tinsley RB, Aprico K, Thorsell A, Nodin C, Nilsson M, Blomstrand F, Eriksson PS. 2006. Reactive astrogliosis induces astrocytic differentiation of adult neural stem/progenitor cells in vitro. J Neurosci Res 84:1415–1424.

Fawcett JW, Asher RA. 1999. The glial scar and central nervous system repair. Brain Res Bull 49:377–391.

Ferreira A, Busciglio J, Caceres A. 1987. An immunocytochemical analysis of the ontogeny of the microtubule-associated proteins MAP-2 and Tau in the nervous system of the rat. Brain Res 431(1):9–31.

Fletcher TL, Cameron P, De Camilli P, Banker G. 1991. The distribution of synapsin I and synaptophysin in hippocampal neurons developing in culture. J Neurosci 11:1617–1626.

Fujimoto ST, Longhi L, Saatman KE, McIntosh TK. 2004. Motor and cognitive function evaluation following experimental traumatic brain injury. Neurosci Biobehav Rev 28:365–378.

Gabbott PL, Stewart MG. 1987. Distribution of neurons and glia in the visual cortex (area 17) of the adult albino rat: a quantitative description. Neuroscience 21:833–845.

Gage FH. 2000. Mammalian neural stem cells. Science 287:1433–1438.

Gary DS, Mattson MP. 2001. Integrin signaling via the PI3-kinase-Akt pathway increases neuronal resistance to glutamate-induced apoptosis. J Neurochem 76:1485–1496.

Gary DS, Milhavet O, Camandola S, Mattson MP. 2003. Essential role for integrin linked kinase in Akt-mediated integrin survival signaling in hippocampal neurons. J Neurochem 84:878–890.

Goedert M, Crowther RA, Garner CC. 1991. Molecular characterization of microtubule-associated proteins tau and MAP2. Trends Neurosci 14:193–199.

Gu Z, Cui J, Brown S, Fridman R, Mobashery S, Strongin AY, Lipton SA. 2005. A highly specific inhibitor of matrix metalloproteinase-9 rescues laminin from proteolysis and neurons from apoptosis in transient focal cerebral ischemia. J Neurosci 25:6401–6408.

Hill SJ, Barbarese E, McIntosh TK. 1996. Regional heterogeneity in the response of astrocytes following traumatic brain injury in the adult rat. J Neuropathol Exp Neurol 55:1221–1229.

Irvin DK, Dhaka A, Hicks C, Weinmaster G, Kornblum HI. 2003. Extrinsic and intrinsic factors governing cell fate in cortical progenitor cultures. Dev Neurosci 25(2–4):162–172.

Kanelos SK, McDeavitt JT. 1998. Neural transplantation: potential role in traumatic brain injury. J Head Trauma Rehabil 13:1–9.

Kobayashi K, Huang C, Lodge T. 1999. Thermoreversible gelation of aqueous methylcellulose solutions. Macromolecules 32:7070–7077.

Kochanek PM, Hendrich KS, Dixon CE, Schiding JK, Williams DS, Ho C. 2002. Cerebral blood flow at one year after controlled cortical impact in rats: assessment by magnetic resonance imaging. J Neurotrauma 19:1029–1037.

Koller H, Siebler M, Schmalenbach C, Muller HW. 1990. GABA and glutamate receptor development of cultured neurons from rat hippocampus, septal region, and neocortex. Synapse 5(1):59–64.

LaPlaca MC, Cullen DK, McLoughlin JJ, Cargill IIRS. 2005. High rate shear strain of three-dimensional neural cell cultures: a new in vitro traumatic brain injury model. J Biomech 38:1093–1105.

Leone DP, Relvas JB, Campos LS, Hemmi S, Brakebusch C, Fassler R, Ffrench-Constant C, Suter U. 2005. Regulation of neural progenitor proliferation and survival by beta1 integrins. J Cell Sci 118(Pt 12): 2589–2599.

Li JH, Wang YH, Wolfe BB, Krueger KE, Corsi L, Stocca G, Vicini S. 1998. Developmental changes in localization of NMDA receptor subunits in primary cultures of cortical neurons. Eur J Neurosci 10:1704–1715.

Logan A, Berry M, Gonzalez AM, Frautschy SA, Sporn MB, Baird A. 1994. Effects of transforming growth factor beta 1 on scar production in the injured central nervous system of the rat. Eur J Neurosci 6:355–363.

Longhi L, Zanier ER, Royo N, Stocchetti N, McIntosh TK. 2005. Stem cell transplantation as a therapeutic strategy for traumatic brain injury. Transpl Immunol 15(2):143–148.

Lu P, Jones LL, Snyder EY, Tuszynski MH. 2003. Neural stem cells constitutively secrete neurotrophic factors and promote extensive host axonal growth after spinal cord injury. Exp Neurol 181(2):115–129.

Margulies SS, Thibault LE, Gennarelli TA. 1990. Physical model simulations of brain injury in the primate. J Biomech 23:823–836.

McCarthy KD, de Vellis J. 1980. Preparation of separate astroglial and oligodendroglial cell cultures from rat cerebral tissue. J Cell Biol 85:890–902.

McGraw J, Hiebert GW, Steeves JD. 2001. Modulating astrogliosis after neurotrauma. J Neurosci Res 63(2):109–115.

McIntosh TK, Juhler M, Raghupathi R, Saatman KE, Smith DH. 1999. Secondary brain injury: neurochemical and cellular mediators. Traumatic brain injury.

McKeon RJ, Jurynec MJ, Buck CR. 1999. The chondroitin sulfate proteoglycans neurocan and phosphacan are expressed by reactive astrocytes in the chronic CNS glial scar. J Neurosci 19:10778–10788.

Meaney DF, Smith DH, Shreiber DI, Bain AC, Miller RT, Ross DT, Gennarelli TA. 1995. Biomechanical analysis of experimental diffuse axonal injury. J Neurotrauma 12:689–694.

Micci MA, Pattillo MT, Kahrig KM, Pasricha PJ. 2005. Caspase inhibition increases survival of neural stem cells in the gastrointestinal tract. Neurogastroenterol Motil 17:557–564.

Mondal D, Pradhan L, LaRussa VF. 2004. Signal transduction pathways involved in the lineage-differentiation of NSCs: can the knowledge gained from blood be used in the brain? Cancer Invest 22:925–943.

Morgenstern DA, Asher RA, Fawcett JW. 2002. Chondroitin sulphate proteoglycans in the CNS injury response. Prog Brain Res 137:313–332.

Nunez J. 1988. Immature and mature variants of MAP2 and tau proteins and neuronal plasticity. Trends Neurosci 11:477–479.

Passaquin AC, Schreier WA, de Vellis J. 1994. Gene expression in astrocytes is affected by subculture. Int J Dev Neurosci 12:363–372.

Picard-Riera N, Nait-Oumesmar B, Baron-Van Evercooren A. 2004. Endogenous adult neural stem cells: limits and potential to repair the injured central nervous system. J Neurosci Res 76:223–231.

Pizzi M, Valerio A, Belloni M, Arrighi V, Alberici A, Liberini P, Spano P, Memo M. 1995. Differential expression of fetal and mature tau isoforms in primary cultures of rat cerebellar granule cells during differentiation in vitro. Brain Res Mol Brain Res 34(1):38–44.

Povlishock JT, Katz DI. 2005. Update of neuropathology and neurological recovery after traumatic brain injury. J Head Trauma Rehabil 20(1): 76–94.

Raghupathi R. 2004. Cell death mechanisms following traumatic brain injury. Brain Pathol 14:215–222.

Rao MS. 1999. Multipotent and restricted precursors in the central nervous system. Anat Rec 257:137–148.

Ray SK, Dixon CE, Banik NL. 2002. Molecular mechanisms in the pathogenesis of traumatic brain injury. Histol Histopathol 17:1137–1152.

Riess P, Zhang C, Saatman KE, Laurer HL, Longhi LG, Raghupathi R, Lenzlinger PM, Lifshitz J, Boockvar J, Neugebauer E, Snyder EY, McIntosh TK. 2002. Transplanted neural stem cells survive, differentiate, and improve neurological motor function after experimental traumatic brain injury. Neurosurgery 51:1043–1052; discussion 1052–1044.

Santa-Olalla J, Covarrubias L. 1995. Epidermal growth factor (EGF), transforming growth factor-alpha (TGF-alpha), and basic fibroblast growth factor (bFGF) differentially influence neural precursor cells of mouse embryonic mesencephalon. J Neurosci Res 42:172–183.

Schmeichel KL, Bissell MJ. 2003. Modeling tissue-specific signaling and organ function in three dimensions. J Cell Sci 116(Pt 12):2377–2388.

Shear DA, Tate MC, Archer DR, Hoffman SW, Hulce VD, Laplaca MC, Stein DG. 2004. Neural progenitor cell transplants promote long-term functional recovery after traumatic brain injury. Brain Res 1026(1):11–22.

Shindo T, Matsumoto Y, Wang Q, Kawai N, Tamiya T, Nagao S. 2006. Differences in the neuronal stem cells survival, neuronal differentiation and neurological improvement after transplantation of neural stem cells between mild and severe experimental traumatic brain injury. J Med Invest 53(1–2):42–51.

Smith DH, Chen XH, Pierce JE, Wolf JA, Trojanowski JQ, Graham DI, McIntosh TK. 1997. Progressive atrophy and neuron death for one year following brain trauma in the rat. J Neurotrauma 14:715–727.

Smith GM, Rutishauser U, Silver J, Miller RH. 1990. Maturation of astrocytes in vitro alters the extent and molecular basis of neurite outgrowth. Dev Biol 138:377–390.

Stabenfeldt SE, Garcia AJ, LaPlaca MC. 2006. Thermoreversible laminin-functionalized hydrogel for neural tissue engineering. J Biomed Mater Res A 77:718–725.

Steinschneider R, Delmas P, Nedelec J, Gola M, Bernard D, Boucraut J. 1996. Appearance of neurofilament subunit epitopes correlates with electrophysiological maturation in cortical embryonic neurons cocultured with mature astrocytes. Brain Res Dev Brain Res 95(1):15–27.

Tate MC, Garcia AJ, Keselowsky BG, Schumm MA, Archer DR, LaPlaca MC. 2004. Specific beta1 integrins mediate adhesion, migration, and differentiation of neural progenitors derived from the embryonic striatum. Mol Cell Neurosci 27(1):22–31.

Tate MC, Shear DA, Hoffman SW, Stein DG, Archer DR, LaPlaca MC. 2002. Fibronectin promotes survival and migration of primary neural stem cells transplanted into the traumatically injured mouse brain. Cell Transplant 11:283–295.

Tate MC, Shear DA, Hoffman SW, Stein DG, LaPlaca MC. 2001. Biocompatibility of methylcellulose-based constructs designed for intracerebral gelation following experimental traumatic brain injury. Biomaterials 22:1113–1123.

Tom VJ, Doller CM, Malouf AT, Silver J. 2004. Astrocyte-associated fibronectin is critical for axonal regeneration in adult white matter. J Neurosci 24:9282–9290.

Weber JT. 2004. Calcium homeostasis following traumatic neuronal injury. Curr Neurovasc Res 1(2):151–171.

Whittemore SR. 1999. Neuronal replacement strategies for spinal cord injury. J Neurotrauma 16:667–673.

Yamada KM, Pankov R, Cukierman E. 2003. Dimensions and dynamics in integrin function. Braz J Med Biol Res 36:959–966.